Engineering Structures 292 (2023) 116585

Contents lists available at ScienceDirect

Engineering Structures

journal homepage: www.elsevier.com/locate/engstruct

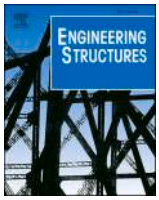

Long-term flexural response of reinforced calcium sulfoaluminate/cement concrete beams

Marianovella Leone [a], Gianni Blasi [a,*], Daniele Colonna [b]

[a] Department of Engineering for Innovation, University of Salento, Italy
[b] Freelance Civil Engineer, Italy

ARTICLE INFO

Keywords:
CSA binder
Experimental test
RC frames
Long-term response

ABSTRACT

Calcium sulfoaluminate binder is an up-to-date solution for reducing the environmental impact of construction industry. Several studies showed satisfactory mechanical performance of concrete realized with such binder, as well as a significant CO_2 emission reduction compared to ordinary Portland cement. However, a lack of knowledge on the mechanical behaviour of calcium sulfoaluminate concrete elements still exists. Particularly, a limited number of studies on long-term mechanical response is available in the literature. In this work, an investigation on full-scaled reinforced concrete beams made of calcium sulfoaluminate binder is reported, aiming at analysing their long-term response in loaded and un-loaded conditions. Two sets of beams, with different calcium sulfoaluminate and ordinary Portland cement percentage were realized. In the first set, serviceability performance level load was applied, while no loading condition was considered in the second set. Both sets were subjected to long-term exposure in ordinary environment and subsequently tested through four point-bending loading up to failure. The non-linear load–deflection response was deeply analysed alongside that of virtually identical unexposed beams tested in a previous experimental campaign. The experimental results were compared to analytical predictions to assess the reliability of existing formulations in reproducing short- and long-term behaviour. A satisfactory long-term performance of the beams realized using calcium sulfoaluminate binder was observed, confirming the suitability of this technology for structural applications. On the other hand, results evidenced the need of updating existing analytical formulations to accurately predict deformation capacity and crack pattern in calcium sulfoaluminate binder elements.

1. Introduction

Past studies have shown the high contribution of cement manufacturing to environmental pollution, particularly referring to CO_2 emissions [1,2]. In fact, production of cement mixtures generates the highest amount of CO_2 amongst all industrial processes, namely 5–7% of the annual man-made global CO_2 emissions [3,4]. In this process, 50% of the CO_2 is released by calcination of limestone and 43% by fuel combustion [5]. Ordinary Portland Cement (OPC) is by far the most widely adopted binder and its employment will likely rise by 2030, due to the increasing construction industry demand in developing Countries [6,7]. This fashion has triggered the attention of the scientific community on the need of developing alternative environmental-friendly cementitious materials and binders [8,9]. To this regard, one of the up-to-date solutions is calcium sulfoaluminate binder (CSA) [10]. CSA is produced by relative-low temperature combustion of raw metal composed of limestone, bauxite and anhydrite, and subsequent addition of gypsum [11]. The lower combustion temperature and amount of limestone compared to OPC allows reducing CO_2 emissions by 25–35%.

CSA has been recently employed in several contexts, such as bridges, concrete pipes, precast concrete frame elements and waterproof layers [12]. Its alkalinity (pH between 10 and 11.5) and porosity, as well as the formation of ettringite and the AFm phases [13], which bind with heavy metals, also leads to suitability for hazardous waste encapsulation [14–16] and glass-fibre reinforced concrete (GFRC) applications [17]. Past studies showed faster setting and hardening of CSA compared to OPC, which lead to rapid achievement of high mechanical strength of concrete. Additionally, greater compressive strength is generally obtained using CSA compared to OPC [18,19]. Several advantages compared to OPC were also detected referring to physical properties of CSA, such as significantly higher and more rapidly achieved heat of hydration [20] and lower volume change when exposed to sulfuric acid

* Corresponding author.
E-mail address: gianni.blasi@unisalento.it (G. Blasi).

https://doi.org/10.1016/j.engstruct.2023.116585
Received 27 February 2023; Received in revised form 3 June 2023; Accepted 8 July 2023

[21]. Furthermore, early hydration reduces creep and drying shrinkage in such binders [22,23], suggesting greater long-term performance compared to OPC. On the other hand, a number of studies showed lower chloride penetration resistance in CSA [24], which may lead to faster corrosion of rebars in case of employment for RC elements.

Experimental tests on full scaled RC beams were also performed, to compare the flexural response in case of CSA and OPC binder employment [25]. The tests showed a similar overall response between the two mixtures, particularly referring to cracking behaviour. Additionally, higher ductility was observed in case of CSA binder, confirming its reliability for structural application.

Despite several advantages from a mechanical and chemical standpoint, the higher cost of raw materials employed in CSA compared to OPC [26] discourages its widespread use in construction industry, leading to the continuous search for more effective solutions [27–31]. Generally, OPC and CSA blending is adopted to reduce costs, although lower short-term compression strength, larger pore generation and higher carbonation depth can be obtained compared to plain CSA [16]. On the other hand, a further increase of the compressive strength at long-term was observed [32].

Although CSA binder shows satisfactory mechanical properties, lack of knowledge is still detected on several aspects, such as the correlation between Young's modulus and compressive strength [33], as well as the long-term behaviour of reinforced concrete (RC) elements realized with such binder. Therefore, comprehensive studies are required on RC elements realized using CSA or CSA-OPC combination, investigating long-term behaviour. The results discussed in this paper are part of a broader experimental campaign [23], aimed at comparing the performance of OPC and CSA. Long-term mechanical response under bending of full-scaled RC beams, realized using the concretes mixtures discussed in depth in [23], was analysed. The RC beams were exposed for 462 days to outdoor ordinary environment and were subjected to constant four-point bending load using an experimental set-up "ad-hoc" designed for replicating in-life service conditions. Additional RC beams with no applied load were exposed to the same environment. After the exposure period, four point bending tests were performed to assess the flexural behaviour up to failure and the crack pattern evolution. The crack width values obtained from the tests were compared to those derived from the consolidated formulation provided in Model Code 2010 [34]. Lastly, the long-term response was compared to short-term response analysed in [23], in order to evaluate the influence of the concrete mixture, environmental conditions and service loads on the performance. The results showed similar response when comparing all the considered specimens, although higher influence of long-term loading was observed in case of blended OPC/CSA beams with low CSA content. On the other hand, higher CSA content in binder reduced creep and drying shrinkage phenomena, leading to greater stiffness and different cracking response.

2. Physical and mechanical proPerties of concrete mixtures

The properties at fresh and hardened state of five concrete mixtures made using OPC and CSA were investigated. Three mixtures were realized blending OPC and CSA, while only OPC was employed for the remaining two mixtures. In Table 1, the details of the mix design for each mixture are provided. The first two numbers in the mixture ID refer to the percentage amount in weight of ordinary Portland cement and calcium sulfoaluminate cement, respectively. The OPC+ mixture was obtained by adding gypsum and reducing the water/binder ratio. Both CSA and OPC were produced by Italcementi Group (i.tech ALI CEM Green® and Cem II A/LL 42.5®, respectively). Particularly, CSA binder was composed of aluminium source (37.53%), limestone (31.86%), gypsum sources (30.32%) and other components (0.28%), as declared by the manufacture's Environmental Product Declaration (EPD).

Polycarboxylate-based admixture was used as plasticizer, while lithium carbonate and citric acid were used as set inductor and retarder. The mixtures were realized using a total cement amount of 340 kg/m^3 and a water/cement ratio ($\boldsymbol{w/c}$) equal to 0.5, except for OPC+. The fresh concrete proprieties were estimated in terms of slump value [35], class of consistency [36] and percentage of entrapped air [37]. A more detailed description of the results is provided in Colonna et al. [23]. The hardened concrete properties were evaluated in terms of compressive strength ($\boldsymbol{R_{cm}}$) at 1, 7, 28, 56, 90, 365 and 730 days from casting, by testing 150 mm-side cubic specimens [38]. Additionally, Young's modulus ($\boldsymbol{E_{cm}}$) at 28, 90, 365 and 730 days [39] was computed by compressive tests on cylinders with diameter and height equal to 150 mm and 300 mm, respectively. All the samples were cast in steel moulds, vibrated and stored for 24 h, using plastic sheets as cover. Afterwards, the samples were demoulded and stored in climatic chamber (20 ± 2 °C and RH > 95%) for 28 days. Tables 2 and 3 provide the value of compressive strength and secant modulus of elasticity at each time frame ($\boldsymbol{R_{cm,t}}$ and $\boldsymbol{E_{cm,t}}$, respectively), alongside their ratio to the values at 28 days ($\boldsymbol{R_{cm,28}}$ and $\boldsymbol{E_{cm,28}}$, respectively).

In case of blended OPC/CSA, a higher curing after 28 days was detected compared to OPC. $\boldsymbol{R_{cm}}$ increased by 41% and 56% from day 28 to day 730 for 70/30OPC/CSA and 50/50OPC/CSA, respectively, while a 31% increase was observed for OPC. However, the opposite trend was observed up to 28 days. In fact, $\boldsymbol{R_{cm}}$ of OPC and OPC+ after 7 days is equal to 90% of $\boldsymbol{R_{cm,28}}$, while it ranges between 62% and 74% of $\boldsymbol{R_{cm,28}}$ in the case of 70/30 OPC/CSA and 50/50 OPC/CSA, respectively (Table 2).

Referring to 100CSA, a faster compressive strength increase was obtained up to 28 days compared to blended OPC/CSA. On the other hand, a 12% increase between 28 and 730 days was obtained. The

Table 1
Concrete mix-design.

MATERIALS [kg/m^3]	OPC	OPC+	70/30 OPC/CSA	50/50 OPC/CSA	100CSA
Sand (0.2–0.35)	270	253	269	268	269
Sand (0.6–1.0)	206	193	205	205	205
Sand (1.5–2.5)	275	257	273	273	273
Sand (3.0–4.0)	149	136	148	148	148
Gravel (6.0–10.0)	351	328	349	348	349
Gravel (10.0–20.0)	612	572	608	607	608
ALICEM	–	–	102	170	340
CEM II A-LL 42.5 R	340	450	238	170	–
Plasticizers	1.20	1.85	1.10	2.25	1.30
Citric acid	–	–	1.36	1.36	1.36
Lithium carbonate	–	–	0.34	0.34	0.34
Water/binder	0.50	0.40	0.50	0.50	0.50

Table 2
Evolution of compressive strength with time for all the considered binders [23].

Mix	$R_{cm,t}$ [MPa] ($R_{cm,t}/R_{cm,28}$)						
	Day						
	1	7	28	56	90	365	730
OPC	18 (0.51)	32.1 (0.90)	35.6 (1.00)	38.5 (1.08)	37.6 (1.06)	42.1 (1.18)	46.8 (1.31)
OPC+	29.6 (0.65)	41.2 (0.90)	45.8 (1.00)	48.7 (1.06)	48.6 (1.06)	54.4 (1.19)	61.6 (1.34)
70/30 OPC/CSA	20.8 (0.47)	27.5 (0.62)	44.1 (1.00)	49.5 (1.12)	53.6 (1.22)	60.1 (1.36)	62.3 (1.41)
50/50 OPC/CSA	28.4 (0.58)	36.1 (0.74)	49.1 (1.00)	60.5 (1.23)	63.4 (1.29)	69.1 (1.41)	76.5 (1.56)
100CSA	43.8 (0.70)	55.8 (0.89)	62.6 (1.00)	64.1 (1.02)	66.7 (1.07)	72.0 (1.15)	70.1 (1.12)

Table 3
Evolution of Young's modulus with time for all the considered binders [23].

Mix	$E_{cm,t}$ [GPa] ($E_{cm,t}/E_{cm,28}$)			
	Day			
	28	90	365	730
OPC	28.7 (1.00)	30.9 (1.08)	30.1 (1.05)	32.5 (1.13)
OPC+	29.6 (1.00)	30.2 (1.02)	31.5 (1.06)	33.2 (1.12)
70/30 OPC/CSA	28.8 (1.00)	29.1 (1.01)	31.2 (1.08)	31.1 (1.08)
50/50 OPC/CSA	29.8 (1.00)	32.0 (1.07)	32.7 (1.10)	32.1 (1.08)
100CSA	31.6 (1.00)	32.6 (1.03)	35.8 (1.13)	34.4 (1.09)

results may suggest that the use of OPC/CSA blend leads to slow-curing concrete, while fast curing is obtained when adopting pure CSA binder.

Additionally, higher compressive strength can be obtained for blended OPC/CSA mixtures compared to OPC. In fact, the highest and lowest compressive strength at 730 days was obtained for 50/50CSA concrete and OPC concrete, respectively (76.5 MPa and 46.8 MPa, respectively). Moreover, the $\boldsymbol{R_{cm}}$ at 730 days for 100CSA (70.1 MPa) was 49.7% higher compared to that obtained for OPC (46.8 MPa), confirming the high suitability of CSA binder as an alternative "green" solution.

Referring to elastic modulus, similar values were obtained comparing all the considered mixtures. in fact, $\boldsymbol{E_{cm}}$ increases by 1–8% and 8–13% after 90 and 730 days, respectively. However, the statement above regarding the different compressive strength increase rate between the analysed mixtures can not be applied to the elastic modulus. Differently from the case of $\boldsymbol{R_{cm}}$, no significant difference was detected in terms of Young's modulus evolution with time comparing the analysed mixtures. The value of $\boldsymbol{E_{cm}}$ at 730 ranged between 31.1 GPa for 70/30OPC/CSA and 34.4 GPa for 100CSA.

Creep and drying shrinkage tests were also performed for the considered mixtures, except for the case of OPC+. The samples realized for creep tests had dimensions equal to 120 × 120 × 360 mm^3 and were stored in a climatic chamber with 20 ± 0.5 °C and 57 ± 3% relative humidity. Additionally, axial load equal to 10% of the compressive strength was applied to the samples. Referring to drying shrinkage tests, 120 × 120 × 360 mm^3 samples were realized and stored in climatic chamber at 20 ± 0.5 °C and RH ≥ 95% for 24 h. Afterwards, the environmental parameters were set to 20 °C and 57% RH, to measure drying shrinkage over time. The results of the tests are provided in Fig. 1**a** and **b**, respectively. A noticeable influence of the binder type on both creep and drying shrinkage was detected, although the relationship with CSA/OPC ratio seems unclear. In fact, greater performances were observed for 50/50 OPC/CSA and 100CSA compared to OPC, while a different trend is observed for 70/30 OPC/CSA.

3. Long-term flexural behaviour of RC beams

Aiming to assess the long-term performance of structural elements realized with OPC/CSA binders, three sets of RC beams were realized using five concrete mixtures for each set, namely C50/50, C70/30, C100, OPC and OPC +. Full-scaled specimens with span equal to 2.8 m and cross-sectional area equal to 200 mm × 200 mm were tested. The longitudinal reinforcement was composed of 2 + 4 (compression + tension) steel rebars with diameter equal to 14 mm. The transverse reinforcement was composed of 8 mm stirrups with spacing equal to 70 mm and 140 mm within the shear span and the constant moment region, respectively. The yielding strength $\boldsymbol{f_y}$ and the ultimate tensile strength $\boldsymbol{f_u}$ of steel were equal to 499 MPa and 604 MPa, respectively, for longitudinal rebars, and 490 MPa and 578 MPa, respectively, for transverse rebars. Nominal concrete cover depth was equal to 30 mm.

The RC beams in the first two sets were exposed for 462 days to outdoor ordinary environment in the area of Lecce (Italy) and were subjected to constant four-point bending load through an *ad hoc* designed experimental set-up. The applied load was equal to 40 kN, corresponding to the 44% of the expected ultimate load for the reference beam made with OPC. These sets are referred as LL (Long-term Loaded) in the following. The RC beams in the third set were subjected to the same environmental condition for the same period, without any applied load. This set of beams is referred as LUN (Long-term Un-Loaded) in the following. After 462 days of outdoor exposure, the first set of LL beams and LUN beams were subjected to four-point bending tests up to failure. The response of the beams was monitored during the test in terms of bending moment, deflection, concrete and steel rebar strain at the mid-span cross-section and crack pattern. The results of LL beams were compared to those of LUN beams, aiming to assess the effect of service loads. Additionally, the long-term response obtained in this work was compared to the short-term response obtained on virtually identical beams analysed in [23].

For sake of clarity, the IDs used in the following to address each beam

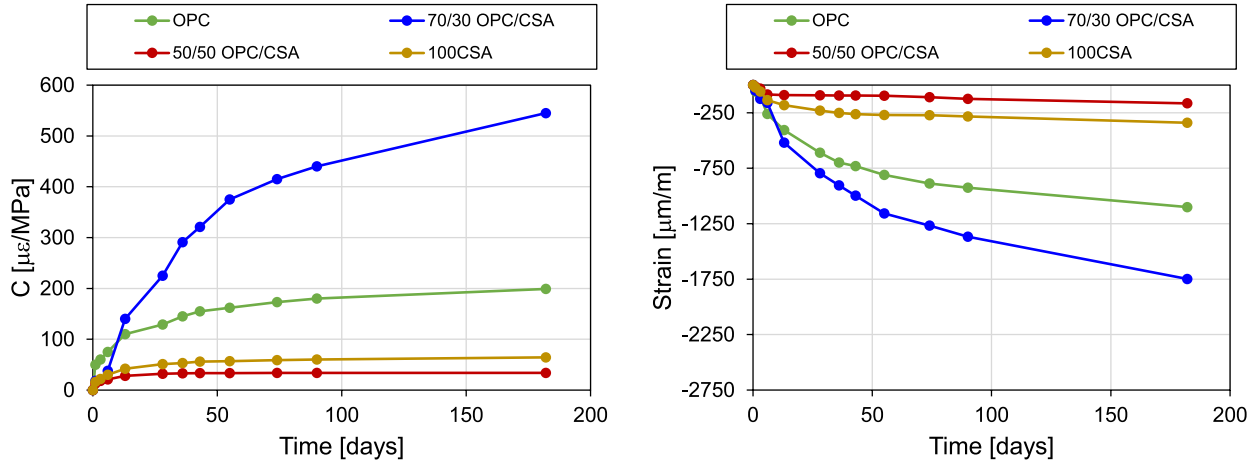

Fig. 1. (a) Creep-vs-time and (b) drying shrinkage vs-time curves for all the considered binders. In fact, this mixture showed both significantly higher creep and drying shrinkage with respect to OPC, suggesting a possible later hydration of the anhydrous OPC cement and relative changes in the microstructure.

tested are composed of a first code, referred to either loaded (LL) or unloaded (LUN) beams, and a second code, referred to the binder used (example: LUN-OPC = Long-term UN-loaded beams with OPC binder; LL-70/30 = Long-term Loaded beams with 70/30OPC/CSA binder).

3.1. Experimental set-up

3.1.1. Long-term loading

The setup used for the long-term loading of the LL beams (Fig. 2) was firstly idealized by Vasanelli et al. [40]. A single contrast steel frame was used to apply the load to a set of five stacked beams. Two supporting steel cylinders were placed between each beam, alternately at the mid span and at the ends, aiming to apply four-point bending to each of the stacked beams. The constant load was applied by mean of mechanical jack, connected to the upper mid-span loading cylinders through a rigid steel beam. The vertical load value was monitored through a load cell placed between the mechanical jack and the contrast frame.

The developed setup was conceived to test five beams at the same time, because of the limitations of lab equipment. Such solution caused a slight variation of the total vertical load among the stacked beams, because of the effect of self-weight. This aspect was addressed in the discussion of the results regarding long-term performance provided in the following.

Crack widening was monitored during the exposure period, employing a digital microscope capable of 60x digital zoom. The crack width for each detected crack was assumed as the average between 18 measured values along the crack length (Fig. 3**a**). Additionally, the deflection of each beam was monitored at three points, corresponding to the mid-span and to the middle of the shear spans. A rectilinear steel rod was placed on the external supports and its relative distance to steel plates tied to the beam was measured through a high precision caliper (Fig. 3b).

In Fig. 3**b**, the values of δ_{1L}, δ_{2L}, δ_{1C}, δ_{2C}, δ_{1R}, δ_{2R}, represent the relative distances between the steel rod and the left (subscript L), centre (subscript C) and right (subscript R) steel plates placed on the upper (subscript 1) and lower (subscript 2) beam, respectively.

3.1.2. Four-point bending tests

The static scheme used in four-point bending tests was virtually identical to that employed during long-term exposure, whilst the testing set-up was modified in order to test a single beam at a time (see Fig. 4). A force-controlled monotonic protocol was used to apply the load to the beam, by employing a hydraulic actuator connected to two loading cylinders through a rigid steel frame. During the test, the vertical displacement of the beam was measured at the mid span, the loading points, the external support points, and at the middle of the shear span. Additionally, maximum concrete and steel strain was monitored in real-time at mid-span, through strain gauges tied to the longitudinal tensile reinforcement and to the compressed concrete side. The cracking pattern was measured in terms of crack length, width, number and spacing, corresponding to four values of vertical load, namely 10 kN, 20 kN, 40 kN and 50 kN. Crack width measurement was conducted as mentioned for the long-term exposure [23].

3.2. Experimental results – Long-term flexural response under constant service load

The evolution of the mid-span deflection of LL beams during the exposure period and the mid-span deflection at 0 (time of load application), 365 and 462 days are provided in Fig. 5**a** and **b**, respectively. It is worth mentioning that the results shown represent the average values computed for the two sets of LL beams. As a general statement, a

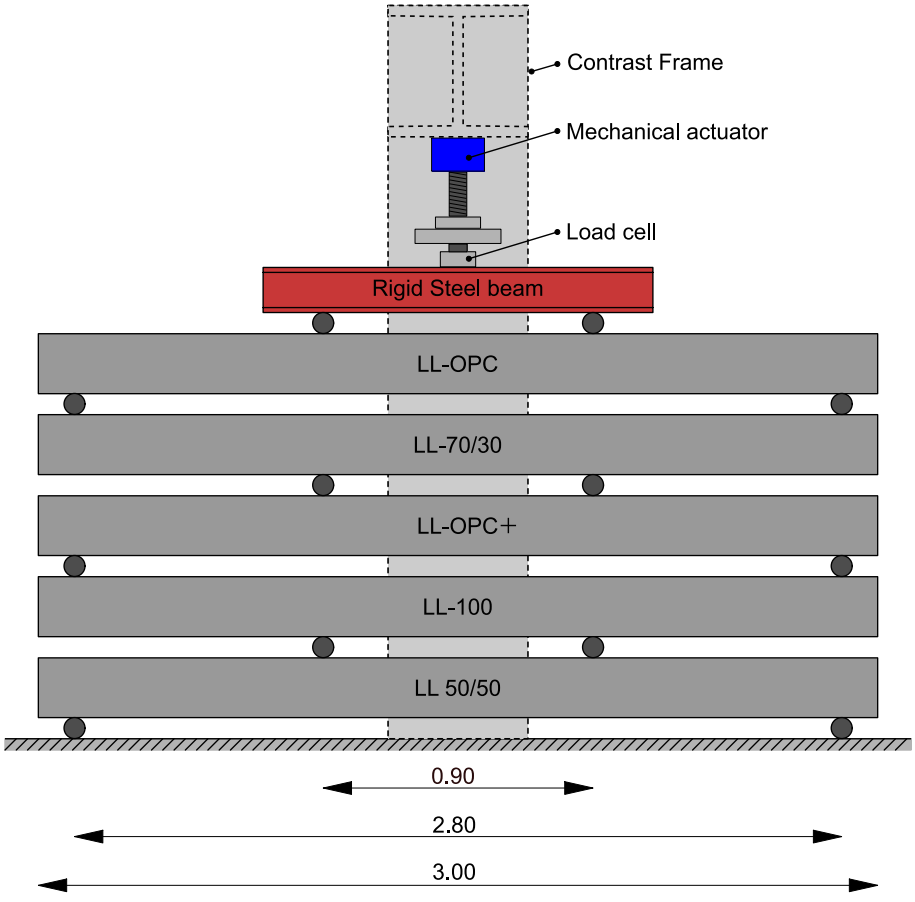

Fig. 2. Long-term bending tests setup.

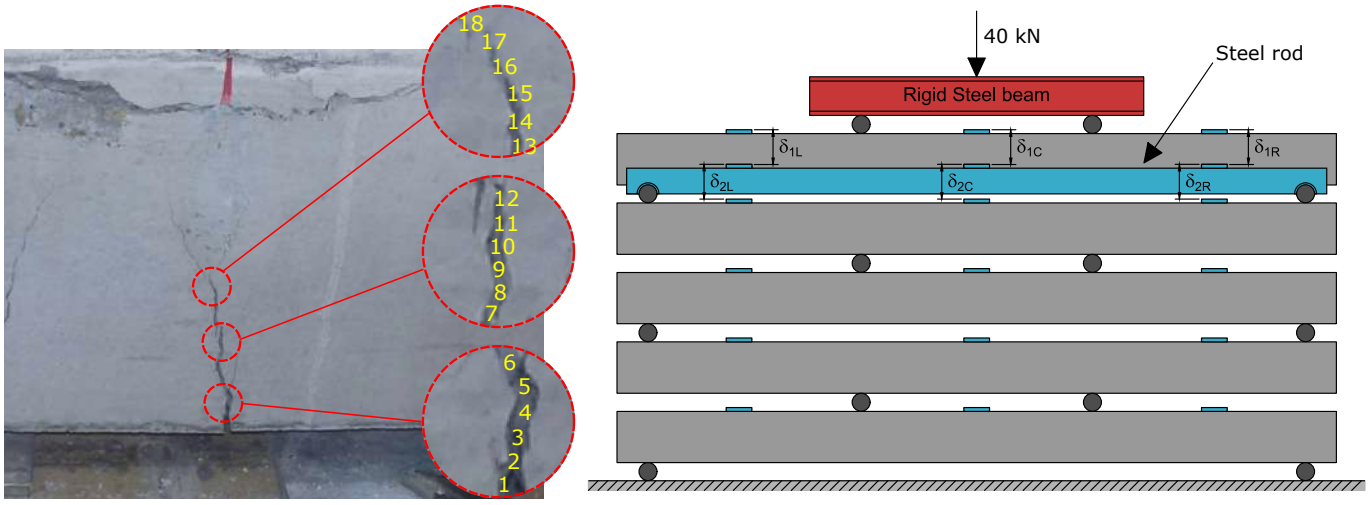

Fig. 3. (a) Crack width and (b) displacement measurement procedure.

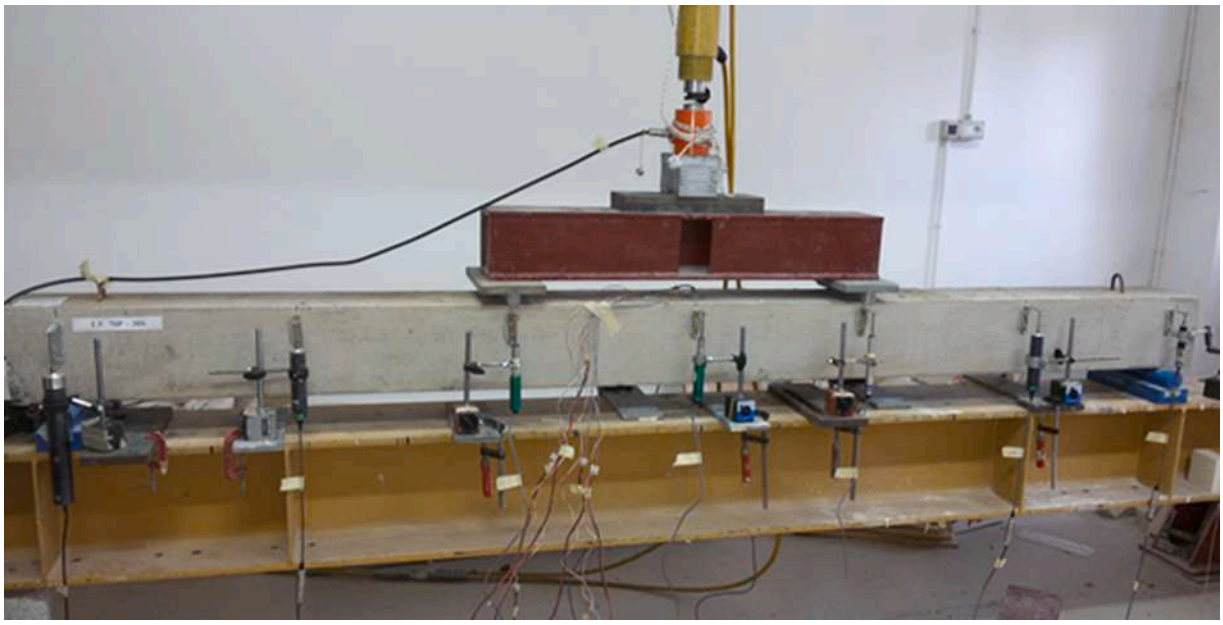

Fig. 4. Experimental set-up for four point bending tests.

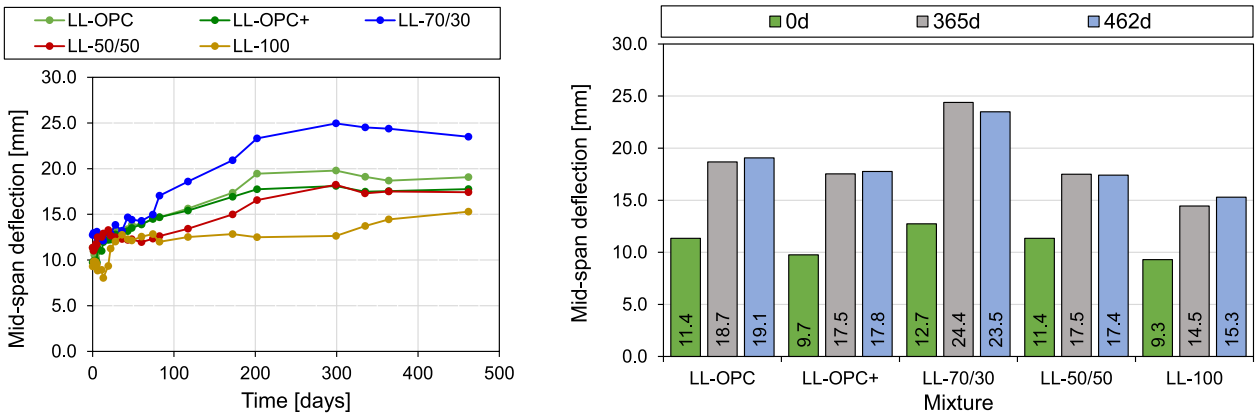

Fig. 5. (a) Mid-span deflection vs exposure time and (b) mid-span deflection at 0, 365 and 462 days.

negligible mid-span deflection increase was observed after 365 days for all the considered specimens. Hence, the binder type seems not to influence the long-term evolution of deflection after one year. A peculiar response was obtained in case of LL-70/30, for which significantly higher deflections were recorded during the exposure period compared to the other specimens. The mid-span deflection at 462 days obtained for LL-70/30 was 54% higher than the lowest value obtained (i.e. LL-100) and 23% higher than that of the OPC beam. This result may be related to higher creep of this specific blended binder, as detected during compression creep tests discussed in [41]. However, a minor influence on the results of the higher load in LL-70/30 compared to OPC (due to self-weight) should be reminded. On the other hand, high content of CSA in binder seems to reduce long-term mid-span deflection, as observed comparing LL-50/50 and LL-100 to OPC and OPC+. This result is even more emphasized when considering higher load on LL-50/50 and LL-100 due to self-weight.

Specimen LL-100 also features a different shape of the deflection-time curve compared to all the remaining specimens. In fact, mid-span deflection significantly increases up to around 30 days, while an almost constant value is observed from 50 to 300 days. This result may be related to higher compressive strength obtained for 100CSA binder (Table 2), which significantly reduces creep effect (also according to [34]). Hence, negligible deflection increase after 30 days is observed. In fact, lower creep was observed for this blend with respect to OPC, caused by faster hydration [42,43], as reported in Fig. 1**a**.

The average crack widening-vs-time curves and the average crack width at 0, 365 and 462 days are provided in Fig. 6**a** and **b**, respectively, referring to the constant bending moment region and averaging the data between the two sets. Additionally, the evolution of average number of cracks in mid-span during the exposure time is reported in Table 4. The average crack width rapidly increased up to 80 days for all the considered specimens, while a lower slope of the curve was observed from 80 to 462 days. Significantly lower values were obtained in case of LL-OPC with respect to all the remaining cases. Particularly, the lower values compared to LL-50/50 and LL-100 seem inconsistent with the results referred to the mid-span deflection (Fig. 5**a**). This fashion may be related, on the one hand, to the higher number of cracks and lower elastic modulus in OPC beam and suggests a more ductile response compared to blended OPC/CSA specimens, (consistently with its lower compressive strength). An in-depth study of the concrete/rebars stress transferring mechanism may assess this scenario. However, no records could be found in the literature to confirm this statement and further investigation is required.

LL-OPC+ beam featured the highest value of average crack width $\boldsymbol{w}$ at 462 days, even though a lower number of cracks was detected compared to LL-OPC. Hence, the reduction of the water/binder ratio (Table 1) may lead to uneven distribution of internal forces and, likely, lower energy dissipation capacity due to more brittle behaviour.

Table 4
Evolution of average number of cracks during exposure time.

Beam	Day						
	1	42	57	75	174	365	462
LL-OPC	8	8.5	8.5	8.5	8.5	8.5	8.5
LL-OPC+	6.5	7	7	7	7	7	7
LL-70/30	8	8	8	8	8	8	8
LL-50/50	7.5	7.5	7.5	7.5	7.5	7.5	7.5
LL-100	7.5	7.5	7.5	7.5	7.5	7.5	7.5

As expected, a great variability of the results is observed for all the considered cases, evidenced by the standard deviation ranges in Fig. 6**b**. Concluding, the presence of CSA or blended OPC/CSA binder seems to penalize the flexural response of RC in terms crack width and number compared to OPC. A different consideration applies to the maximum deflection. In fact, as shown in Fig. 1**a**, low CSA content (LL-70/30) leads to creep increase compared to OPC, while the opposite trend is observed in case of middle-high CSA content (LL-50/50 and LL-100). This feature highlights the hardships in comparing the response of the analysed frames, mainly related to the variability of the width of a single crack along its height. Also in this case, it is worth reminding that LL-OPC was subjected to lower vertical load compared do all the remaining beams. Hence, narrower curves would be obtained when considering identical load to all the beams.

3.3. *Experimental results – four-point bending tests*

The parameters characterising the flexural response of the beams under four-point bending load obtained from the tests are provided in Table 5. Particularly, the yielding strength ($\boldsymbol{F_y}$), the maximum load, $\boldsymbol{F_{max}}$, the corresponding mid-span displacements (δ_y and δ_{max}, respectively), the elastic stiffness ($\boldsymbol{K_{el}}$), the ductility ($\mu = \delta_{max}/\delta_y$), the maximum longitudinal rebars strain (ε_s) and the maximum compressed concrete strain (ε_c) are provided. For sake of clarity, it is worth mentioning that the LL-100 data referred to steel rebars and compressed concrete strain were lost during the test.

As shown in Table 5, the highest and the lowest value of $\boldsymbol{F_{max}}$ for LL beams were obtained in case of LL-50/50 (100.7 kN) and LL-OPC (93.5 kN), respectively. The results obtained for LL-70/30, LL-100 and LL-OPC+ were closer to those referred to LL-50/50 (−3.6%, −0.6% and −1.8%, respectively). A similar trend was observed for LUN beams. This fashion is consistent with the concrete compressive strength results obtained at 365 and 730 days, provided in Colonna et al. [23] and reported in Table 2. In fact, the highest cubic compressive strength was obtained for C50/50 OPC/CSA (76.5 MPa), followed by C100CSA (70.1

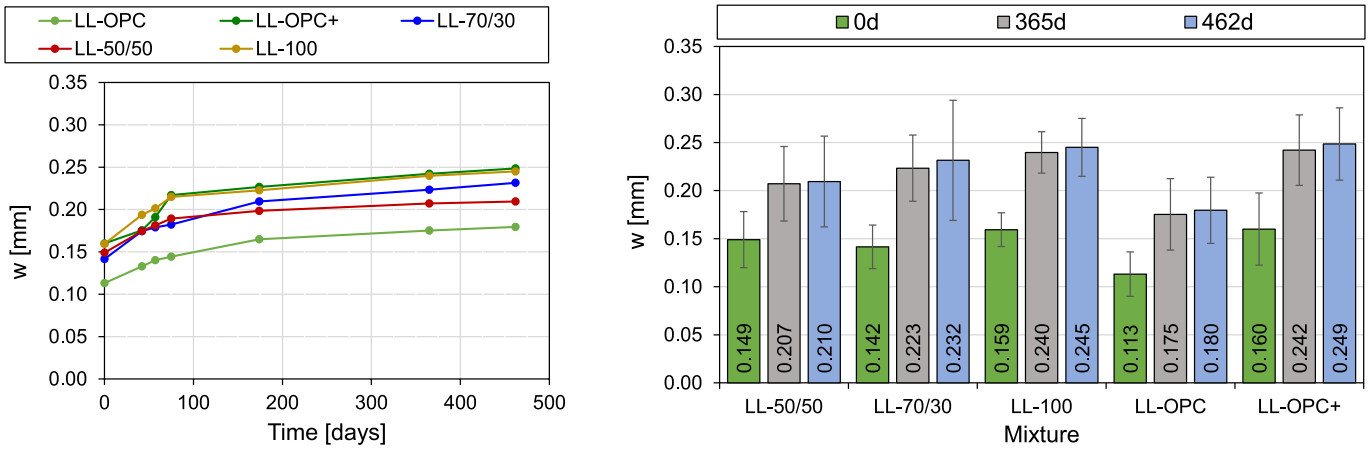

Fig. 6. (a) Mid-span crack widening ($\boldsymbol{w}$) vs exposure time and (b) mid-span crack widening at 0, 365 and 462 days, along with standard deviation ranges.

Table 5
Experimental results referred to four-point bending tests.

Specimen	F_y [kN]	δ_y [mm]	F_{max} [kN]	δ_{max} [mm]	K_{el} [kN/mm]	μ	ε_s	ε_c
LL-OPC	83.90	25.04	93.50	59.92	3.35	2.39	2.4%	3.8‰
LL-OPC+	84.30	22.05	98.90	57.29	3.82	2.60	2.1%	3.2‰
LL-70/30	82.80	28.73	97.10	63.39	2.88	2.21	2.3%	3.1‰
LL-50/50	83.40	18.81	100.70	58.95	4.43	3.13	2.5%	3.2‰
LL-100	86.10	17.18	100.10	43.92	5.01	2.56	–	–
LUN-OPC	88.00	22.45	95.40	44.39	3.92	1.98	2.3	3.4‰
LUN-OPC+	89.40	23.37	99.70	56.09	3.82	2.40	1.8%	3.3‰
LUN-70/30	90.40	23.91	98.60	54.99	3.78	2.30	2.0%	4.1‰
LUN-50/50	90.70	23.80	100.50	51.02	3.81	2.14	2.2%	3.4‰
LUN-100	88.70	22.93	100.40	63.01	3.87	2.75	1.7%	3.5‰

MPa), C70/30 OPC/CSA (62.3 MPa), COPC+ (61.6 MPa) and COPC (46.8 MPa).

For all the tests performed, the failure mechanism of the beams was characterised by mid-span concrete crushing after yielding of the tensile rebars (Fig. 7). This outcome is confirmed by the recorded values of ε_c and ε_s corresponding to the peak load (Table 5). The Load-mid-span displacement relationships obtained from four-point bending tests is provided in Fig. 8**a** and **b** for LUN and LL, respectively. Very close curve shapes were obtained comparing all the considered mixtures in case of LUN (Fig. 8**a**), while a high difference in terms of both pre-yielding shape and ultimate displacement capacity is observed in case of LL beams. Particularly, a significantly lower initial slope was obtained in case of LL-70/30 (Fig. 8**b**) up to a load value equal to 24 kN. Additionally, even after this load level, a lower slope is observed compared to LL-50/50 and LL-100. As a result, the elastic stiffness, computed as $\boldsymbol{K_{el}} = \boldsymbol{F_y}/\delta_{\boldsymbol{y}}$, was significantly lower (-43%) in case of LL-70/30 compared to LL-100, (i.e. the highest value obtained). A similar but less pronounced fashion is observed in case of LL-OPC and LL-OPC+, whose Load-displacement response features a lower slope up to around 14 kN compared to LL-50/50 and LL-100, probably due to lower mechanical performance of the material.

Such difference in LL beams response could confirm creep being more relevant for blended concrete system (OPC/CSA) with low CSA content (e.g. C70/30). On the other hand, lower relaxation was detected in case of CSA content equal or higher than 50% compared to OPC and OPC+ beams. LL results show that CSA mixtures generally provide higher post-cracking stiffness to RC elements compared to OPC mixtures, although no proportional correlation exists between the CSA content and the elastic stiffness. This trend is more evident when considering the response up to 40 kN of applied load (i.e. long-term loading test value).

Fig. 7. Failure mechanism for LL Beams.

It is worth mentioning the higher elastic stiffness obtained in case of LL beams with respect to LUN beams for 50/50 OPC/CSA ad CSA binder. In the authors' opinion, this outcome is only connected to test-to-test variability and can not be intended as a peculiar behaviour for these two blends.

Lastly, the computed ductility for both LL and LUN beams allows to provide information on the influence of the CSA content on the energy dissipation capacity. The relationship between CSA content and ductility seems not clear both in case of LL and LUN beams. In case of LUN beams (Fig. 8**a**), higher ductility was obtained for LUN-100 mixture, while the lowest performance was observed in case of LUN-OPC. Referring to LL beams (Fig. 8**b**) a significant ductility increase was obtained for LL-50/50, while the remaining mixtures provide comparable values of μ. No clear information is obtained comparing LUN to LL beams performance, since exposure time increased the ductility in case of OPC, OPC+ and 50/50 mixture, while a ductility decrease was observed for 70/30 and 100 mixtures.

3.4. Flexural behaviour at short and long-term

A comparison between the load-mid-span deflection response of LL and LUN is provided in Figs. 9, 10, 11 for each mixture considered. Additionally, the short term behaviour of virtually identical beams tested by Colonna et al. [23] is also included in the charts (SL beams), to provide a comprehensive evaluation of the flexural response. This comparison aims to examine the influence of the environmental and in-life service conditions on the flexural behaviour of such elements.

Close results were observed comparing the flexural response at short term (SL) to that at long-term in unloaded conditions (LUN). On the other hand, lower $\boldsymbol{F_m}$ and μ values were obtained for SL beams for almost all the mixtures analysed. In the case of OPC, OPC+ and 70/30 mixture (Figs. 9**a**,**b** and 10**a**, respectively) long-term loading caused lower elastic stiffness in LL beams compared to LUN and SL, as consequence of cracking and creep effect. On the other hand, the opposite trend is observed in case 50/50 and 100 mixtures (Figs. 10**b** and 11, respectively). This result may suggest to test-to-test variability.

The behaviour of blended OPC/CSA concrete specimens highlights that a combination of these two types of binder leads to a reduction of RC elements' performance compared to OPC in case of low amount of CSA, while a sensible increase of the performance may be obtained for a higher CSA content. Concluding, CSA amount equal or higher than 50%, generally leads to a positive influence on the long-term behaviour, caused by both the lower creep deformation and drying shrinkage of the concrete matrix (Fig. 1).

It is worth noting that in the case of 50/50 mixture, a significantly lower performance in terms of maximum strength and ductility was obtained for SL beams comparing to all the remaining analysed cases (Fig. 10**b**). Further investigation is required to provide a clear explanation to this result, although it is not necessarily related to the influence of the mixture and could be caused by specimen's imperfections.

An analytical simulation of four point bending tests was also per-

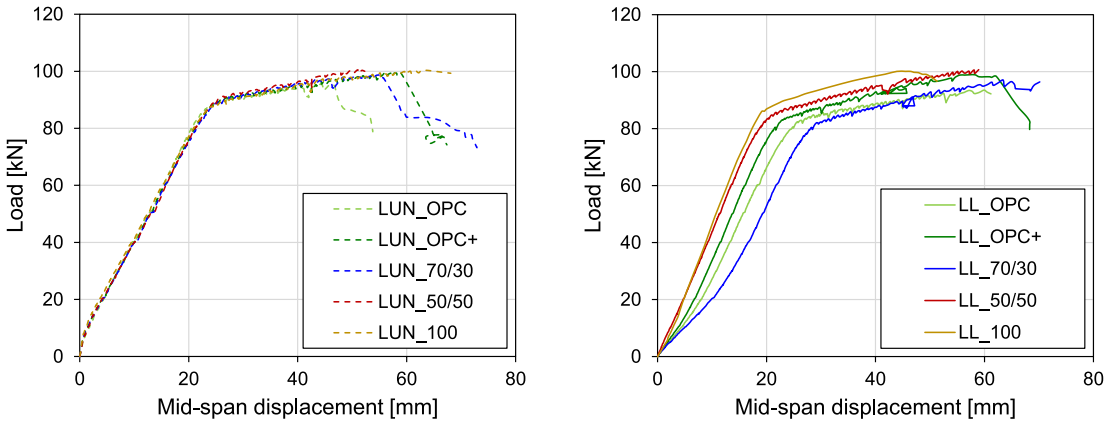

Fig. 8. Force-displacement curves obtained for (a) LUN and (b) LL beams.

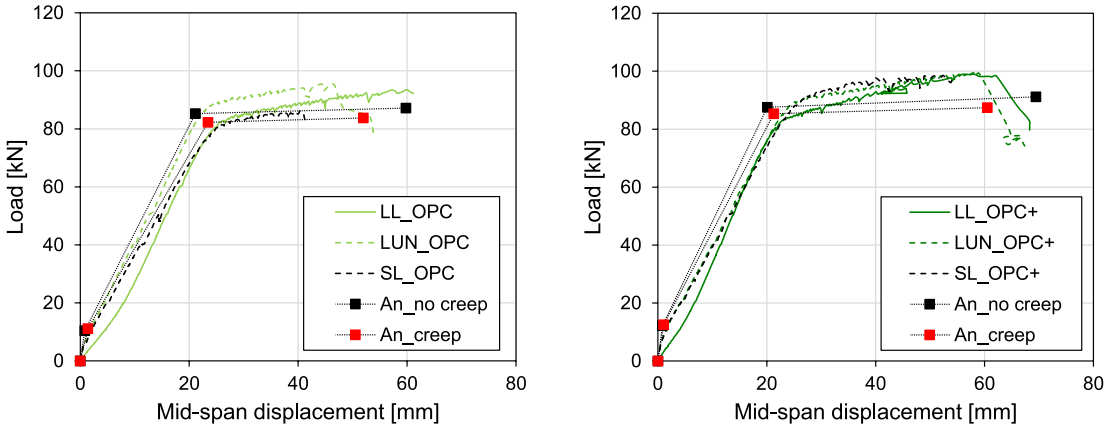

Fig. 9. Comparison between LL, LUN and SL response along with analytical curves for beams with (a) OPC and (b) OPC+ mixtures.

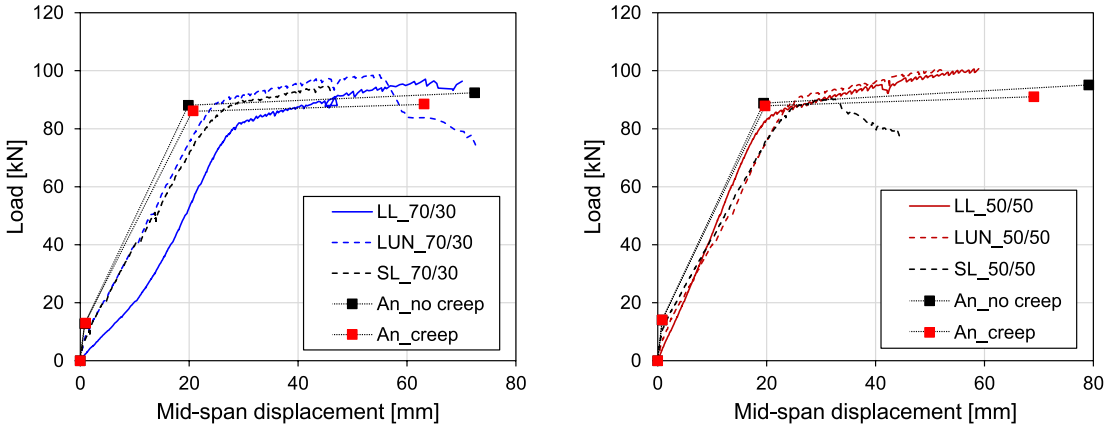

Fig. 10. Comparison between LL, LUN and SL response along with analytical curves for beams with (a) 70/30 and (b) 50/50 mixtures.

formed, whose results are included in Figs. 9, 10, 11. In the analytical model, the load–deflection response was computed based on a trilinear piecewise moment–curvature relationship of the cross-section of the beam. The points of the piecewise curve were defined by computing the resisting moment and the corresponding curvature referred to first cracking, longitudinal bars yielding and ultimate flexural strength, respectively. For each performance level, the internal forces along the cross section were computed considering a fiber approach to define the depth of the neutral axis, assuming elastic-perfectly plastic behaviour for both reinforcing steel and concrete in compression. The length of the plastic hinge considered to obtain load–deflection response from the moment–curvature response was assumed equal to the constant bending moment region of the beam. The analytical results are provided both neglecting and considering long-term creep effects (***An_no creep*** and ***An_creep***, respectively). In the second case, well-known analytical formulations reported in Model Code 10 [34] are employed to compute both compressive strength and Young's modulus at time t ($f_{cm,t}$ and $E_{cm,t}$, respectively):

$$f_{cm,t} = f_{cm,28} \bullet \beta_{c,sus}(t, t_0) \quad (1)$$

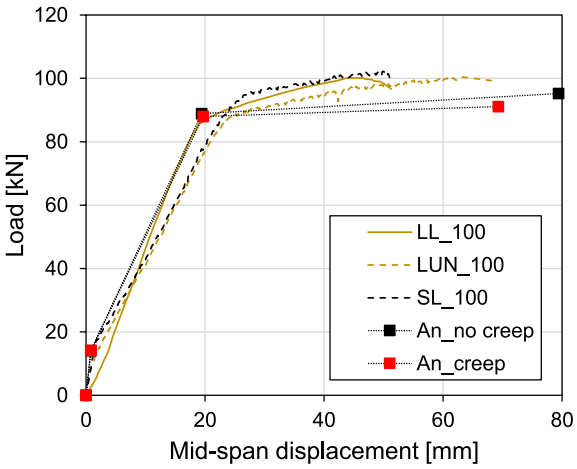

Fig. 11. Comparison between LL, LUN and SL response along with analytical curves for beams with 100CSA mixture.

$$E_{cm,t} = \frac{E_{cm,28}}{\varphi(t,t_0)} \quad (2)$$

In Eqs. (1) and (2), $f_{cm,28}$ and $E_{cm,28}$ are the mean compressive strength and Young's modulus at 28 days, and $\beta_{c,sus}$ is a reduction coefficient accounting for the effects of sustained loads. Additionally, φ is the creep coefficient, depending on compressive strength of concrete and relative humidity. For almost all the specimens, a satisfactory matching between analytical and experimental curves was obtained, particularly in case of LL-OPC. This specific result was expected, because analytical formulations adopted are referred to OPC elements. Analytical long-term effects were negligible for blended OPC/CSA beams, probably due to the high value of concrete compressive strength measured for these cases. In fact, the influence of creep reduces as the compressive strength increases, according to the analytical formulation provided in Model Code 10 [34]. This aspect led to a noticeable mismatch between analytical and experimental curves in case of LL-70/30 (Fig. 10**a**) beam in terms of elastic stiffness. Lastly, an overestimation of the ultimate displacement capacity was obtained in case of 50/50 and 100CSA beams (Figs. 10**b** and 11), probably caused by incorrect blind-estimation of concrete ultimate strain. In fact, higher compressive strength was obtained for such mixtures, which may lead to brittle behaviour in compression. This result could suggest that further investigation is required to analyse long-term response of RC beams with high content of CSA binder, because existing analytical formulations may not provide conservative results.

A summary of the test results obtained in terms of yielding strength, maximum strength, elastic stiffness and ductility is provided in Figs. 12 and 13. Referring to F_y, no significant difference between the mixtures analysed is observed, although a general reduction was obtained comparing LUN/SL to LL beams (Fig. 12**a**). A similar result was obtained for F_m (Fig. 12**b**), even though higher values were observed comparing exposed beams (both LL and LUN) to un-exposed beams. The only exception regards 100CSA mixture, for which the highest F_m value was obtained for SL beams. As a general statement, close F_m values were obtained comparing SL, LUN and LL response for all the mixtures analysed. This outcome suggests a low influence of the CSA content (or cement type) on the flexural strength.

Different observations regard elastic stiffness (Fig. 13**a**). Despite, for SL and LUN beams, no noticeable difference was observed comparing all the specimens, significantly higher elastic stiffness was obtained for LL-50/50 and LL-100 compared to the other beams. Additionally, LL-70/30 features lower stiffness with respect to all the remaining cases, due to higher creep.

Fig. 13**b** reports the ductility values computed for each beam. Both service loads and exposure time increased the value of μ for all considered specimens. This result is due to the higher δ_{max}, which may be related to the greater strain capacity of concrete when creep occurs.

It is worth noting the significantly different response obtained comparing SL, LUN and LL, in the case of C50/50. This specific outcome requires a contextualization, since the higher ductility obtained for LL is the result of its lower yielding strength and higher elastic stiffness compared to SL and LUN. Additionally, anomalous flexural response was obtained for SL, which led to a major reduction of the ultimate deformation.

3.5. Cracking pattern development during four-point bending tests

Cracking patterns detected in the constant bending moment region of the beams during the four-point bending tests are provided in Table 6. The crack widening and number was monitored at four load steps, namely 10, 20, 40 and 50 kN. The average values measured among all the detected cracks are provided for each step, along with the Coefficient of Variation (CoV). Additionally, the difference between crack width measured at 10 and 50 kN ($\Delta_{10\text{-}50}$) is provided. As expected, significantly higher values of crack width were obtained for LL beams, since the presence of service load during the exposure period led to crack generation. This feature justifies the higher increase of crack width in case of LUN beams compared to LL beams during the four-point bending tests. Similar values of $\Delta_{10\text{-}50}$ were obtained for all the considered beams, suggesting that the increase of the crack width up to structural failure is not sensibly influenced by the binder type and long-term loading.

A comparison of the crack development in the constant bending moment region of the beam, between SL, LUN and LL beams, is provided

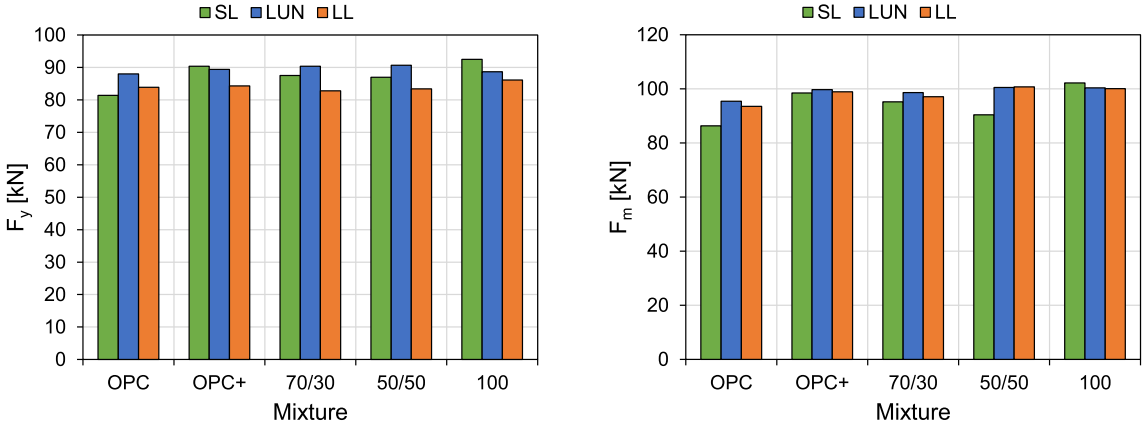

Fig. 12. Comparison between (a) F_y and (b) F_m values obtained over all tested beams.

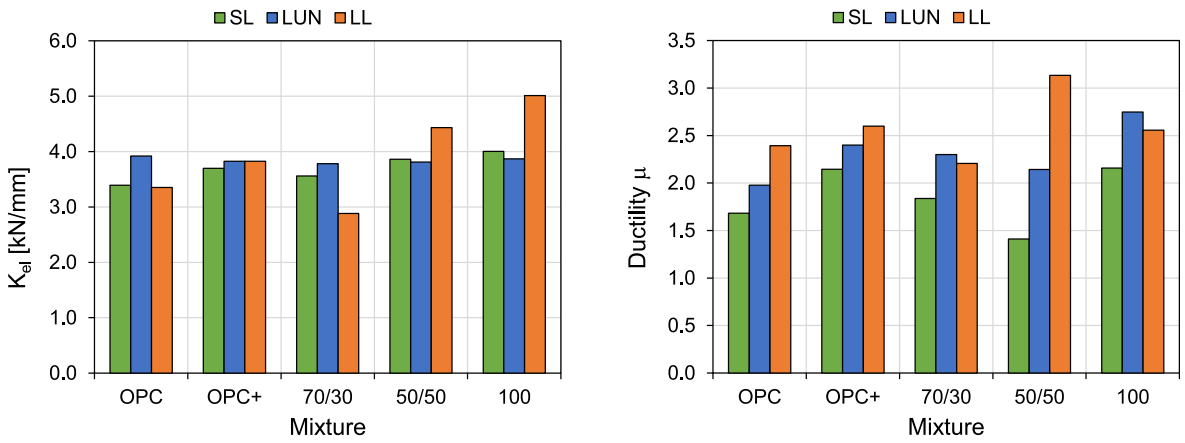

Fig. 13. Comparison between (a) K_{el} and (b) μ values obtained over all tested beams.

Table 6
Crack pattern in the constant bending moment region.

Beam ID	F [kN]	n.	w [mm] (CoV)	$\Delta_{10\text{-}50}$	Beam ID	F [kN]	n.	w [mm] (CoV)	$\Delta_{10\text{-}50}$
LL-OPC	10	9	0.115 (0.16)	0.11	LUN-OPC	10	3	0.031 (0.22)	0.13
	20	9	0.136 (0.13)			20	3	0.054 (0.24)	
	40	9	0.202 (0.12)			40	8	0.126 (0.16)	
	50	9	0.229 (0.13)			50	8	0.165 (0.12)	
LL-OPC+	10	6	0.159 (0.11)	0.15	LUN -OPC+	10	4	0.052 (0.20)	0.12
	20	6	0.201 (0.11)			20	7	0.081 (0.14)	
	40	6	0.269 (0.13)			40	8	0.139 (0.14)	
	50	6	0.306 (0.11)			50	8	0.176 (0.11)	
LL-70/30	10	8	0.142 (0.17)	0.13	LUN −70/30	10	3	0.044 (0.2)	0.15
	20	8	0.163 (0.14)			20	7	0.074 (0.18)	
	40	8	0.240 (0.13)			40	7	0.160 (0.14)	
	50	8	0.268 (0.12)			50	7	0.195 (0.11)	
LL-50/50	10	7	0.151 (0.11)	0.13	LUN −50/50	10	4	0.040 (0.23)	0.10
	20	7	0.167 (0.13)			20	8	0.066 (0.18)	
	40	7	0.230 (0.12)			40	8	0.118 (0.15)	
	50	7	0.277 (0.11)			50	9	0.139 (0.13)	
LL-100	10	8	0.155 (0.16)	0.07	LUN −100	10	2	0.039 (0.31)	0.15
	20	8	0.181 (0.15)			20	7	0.067 (0.17)	
	40	8	0.204 (0.13)			40	7	0.144 (0.13)	
	50	8	0.229 (0.10)			50	7	0.185 (0.11)	

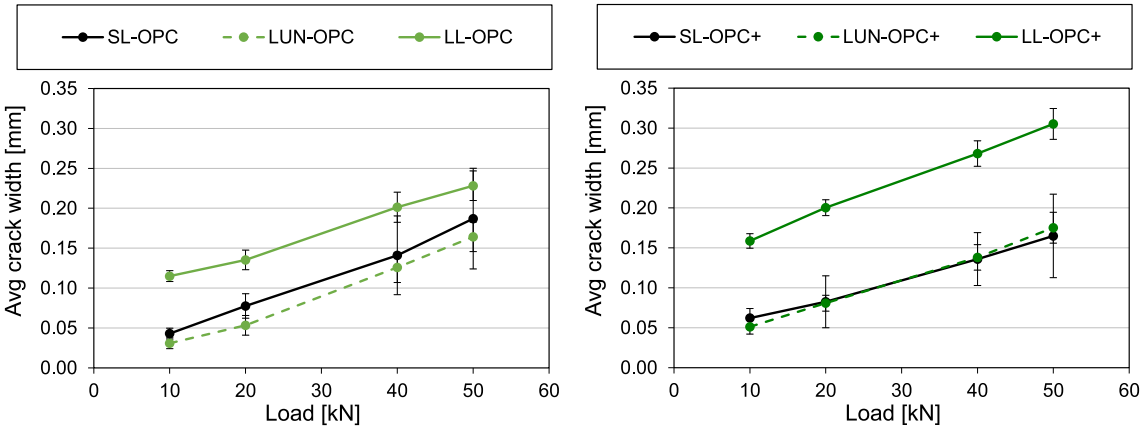

Fig. 14. Comparison between LL, LUN and SL crack widening at mid-span for beams with (a) OPC and (b) OPC + mixtures.

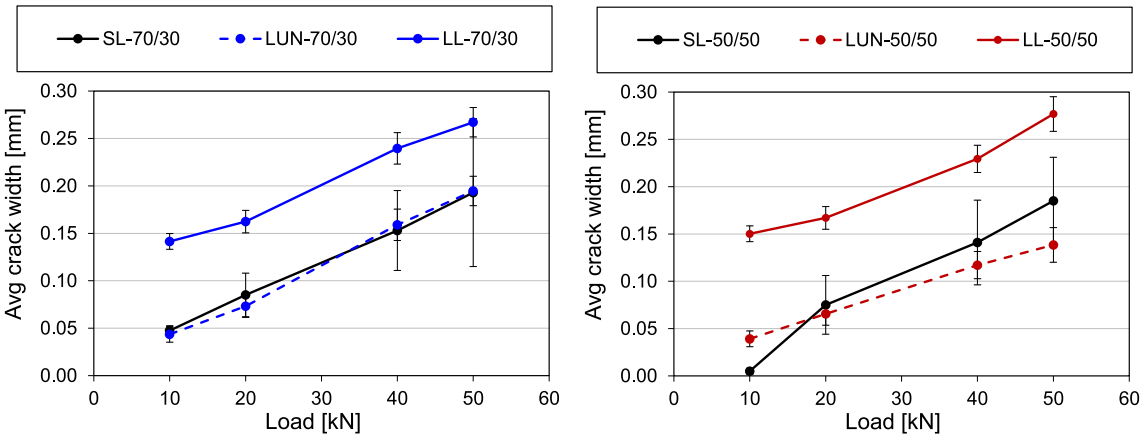

Fig. 15. Comparison between LL, LUN and SL crack widening at mid-span for beams with (a) 70/30 and (b) 50/50 mixtures.

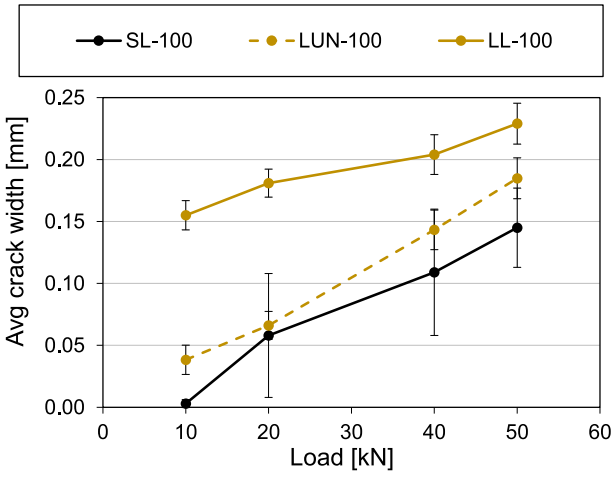

Fig. 16. Comparison between LL, LUN and SL crack widening at mid-span for beams with 100CSA mixture.

for each mixture in Figs. 14, 15, 16. The curves report the values of average crack measured for each of the four load steps, along with the standard deviation. A significant difference is obtained comparing LL beams to SL and LUN beams, consistently with the results referred to Load-displacement response. This outcome highlights the high influence of creep on the flexural response of the beams, regardless of the binder mixture adopted for concrete. Additionally, similar curve slopes were obtained comparing SL, LUN and LL for almost all the considered binder mixtures. Also in this case, 100CSA mixture represents the only exception, since the slope of the curve referred to LL beam is significantly lower than that obtained for SL and LUN, consistently with the higher value of crack width at the end of the exposure period. However, further investigation is required on this mixture to assess whether this outcome could be related to test-to-test variability.

The highest difference between SL and LL average crack width at 50 kN was observed in OPC+ beams (85.0%), while closer values were obtained comparing SL-OPC to LL-OPC (22.0%). It is worth noting the difference between OPC and OPC+ mixture. In fact, significantly higher crack width values were observed in case of OPC+ comparing LL to SL/LUN beams response, while relatively close values were obtained in case of OPC. Additionally, LUN and SL beams feature almost the same response in case of OPC+ (1.6%-21.3% scatter). Referring to OPC/CSA mixtures, 70/30 beams feature higher mid-span crack width compared to 50/50 and 100CSA beams in case of un-loaded condition. Additionally, similar response was obtained comparing LUN-70/30 to SL-70/30, as observed for OPC beams.

4. Conclusions

The need of finding green solutions for reducing the environmental impact of construction industry has been continuously evidenced during last years. Therefore, investigation on state-of-art materials aimed at assessing their reliability for structural applications is still required. The tests performed and discussed in this study were aimed at filling the lack of knowledge on reinforced concrete elements realized using calcium sulfoaluminate binder, focusing on long-term response. The main results of this work are listed in the following:

- A noticeable influence of long-term effects on the mid-span deflection of the beams was observed both in case of ordinary Portland cement and calcium sulfoaluminate binder. For low percentage of calcium sulfoaluminate in binder, a significantly higher deflection was observed compared to the remaining beams, while the lowest deformation was obtained for plain calcium sulfoaluminate in binder.
- A more homogeneous distribution of cracks was observed in case of plain Portland cement beams, featuring a higher number of cracks and lower value of average crack width. This result may suggest that a lower ductility could be obtained for beams realized with blended calcium sulfoaluminate/Portland binder.
- The non-linear force–displacement response obtained through four-point bending tests showed an almost identical response in case of unloaded beams for all the binder types analysed, while a significant difference was observed in case of loaded beams. Additionally, a negligible effect of the binder type on the elastic stiffness was observed comparing unloaded and short-term loaded beams.
- In case of long-term loaded beams, a different fashion was detected. Lower amount of calcium sulfoaluminate in binder led to lower pre-yielding stiffness compared to all the remaining beams. On the other hand, higher content of calcium sulfoaluminate increased flexural stiffness also compared to ordinary Portland cement. This result suggests that concrete creep could be more relevant for blended concrete system with low calcium sulfoaluminate content.
- The analytical simulation of the non-linear response of the beams showed a satisfactory matching between experimental and analytical results, suggesting the reliability of existing formulations also for elements realized using calcium sulfoaluminate binder. On the other hand, the significant increase of compressive strength for such type of binder leads to hardships in simulating long-term effects (e.g. creep) using existing analytical models.

The results obtained herein confirm calcium sulfoaluminate binder being a reliable material for structural applications, showing high strength and stiffness at short-term and similar long-term response

compared to ordinary Portland cement elements. On the other hand, the anomalous response obtained in case of low amount of calcium sulfoaluminate in binder may suggest the accurate design of the ordinary Portland/calcium sulfoaluminate ratio being an aspect of concern.

CRediT authorship contribution statement

Marianovella Leone: Conceptualization, Methodology, Resources, Writing – review & editing, Visualization, Supervision. **Gianni Blasi:** Conceptualization, Methodology, Software, Validation, Formal analysis, Data curation, Writing – review & editing, Visualization. **Daniele Colonna:** Conceptualization, Methodology, Validation, Formal analysis, Investigation, Writing – original draft, Data curation, Visualization.

Declaration of Competing Interest

The authors declare that they have no known competing financial interests or personal relationships that could have appeared to influence the work reported in this paper.

Data availability

Data will be made available on request.

Acknowledgements

The authors gratefully acknowledge HeidelbergCement-ItalCementi group for realizing the specimens tested in this work and for hosting some of the laboratory tests.

References

[1] Le Quéré C, Andres RJ, Boden T, Conway T, Houghton RA, House JI, et al. The global carbon budget 1959–2011. Earth Syst Sci Data 2013;5(1):165–85.
[2] Andrew RM. Global CO2 emissions from cement production, 1928–2018. Earth Syst Sci Data 2019;11(4):1675–710. https://doi.org/10.5194/essd-11-1675-2019.
[3] Ludwig HM, Zhang W. Research review of cement clinker chemistry. Cem Concr Res 2015;78:24–37. https://doi.org/10.1016/j.cemconres.2015.05.018.
[4] Mohamad N, Muthusamy K, Embong R, Kusbiantoro A, Hashim MH. Environmental impact of cement production and Solutions: a review. Mater Today: Proc 2021;48:741–6. https://doi.org/10.1016/j.matpr.2021.02.212.
[5] Hargis CW, Lothenbach B, Müller CJ, Winnefeld F. Carbonation of calcium sulfoaluminate mortars. Cem Concr Compos 2017;80:123–34. https://doi.org/10.1016/j.cemconcomp.2017.03.003.
[6] Müller N, Harnisch J. A blueprint for a climate friendly cement industry; 2008.
[7] Damtoft JS, Lukasik J, Herfort D, Sorrentino D, Gartner EM. Sustainable development and climate change initiatives. Cem Concr Res 2008;38(2):115–27. https://doi.org/10.1016/j.cemconres.2007.09.008.
[8] Abdel Gawwad HA, Abd El-Aleem S, Ouda AS. Preparation and characterization of one-part non-Portland cement. Ceram Int 2016;42(1):220–8. https://doi.org/10.1016/j.ceramint.2015.08.096.
[9] Singh NB, Middendorf B. Geopolymers as an alternative to Portland cement: an overview. Constr Build Mater 2020;237:117455. https://doi.org/10.1016/j.conbuildmat.2019.117455.
[10] Zhang L, Glasser FP, Dyer T. New concretes based on calcium sulfoaluminate cement. Modern Concrete Materials: Binders, Additions and Admixtures; 1999.
[11] Glasser FP, Zhang L. High-performance cement matrices based on calcium sulfoaluminate-belite compositions. Cem Concr Res 2001;31(12):1881–6. https://doi.org/10.1016/S0008-8846(01)00649-4.
[12] Markosian N, Tawadrous R, Mastali M, Thomas RJ, Maguire M. Performance evaluation of a prestressed Belitic Calcium Sulfoaluminate Cement (BCSA) concrete bridge girder nick. Sustainability 2021;13(14). https://doi.org/10.3390/su13147875.
[13] Bertola F, Gastaldi D, Irico S, Paul G, Canonico F. Behavior of blends of CSA and Portland cements in high chloride environment. Constr Build Mater 2020;262:120852. https://doi.org/10.1016/j.conbuildmat.2020.120852.
[14] Juenger MCG, Winnefeld F, Provis JL, Ideker JH. Advances in alternative cementitious binders. Cem Concr Res 2011;41(12):1232–43. https://doi.org/10.1016/j.cemconres.2010.11.012.
[15] Zhou Q, Milestone NB, Hayes M. An alternative to Portland Cement for waste encapsulation-the calcium sulfoaluminate cement system. J Hazard Mater 2006;136(1 SPEC. ISS.):120–9. https://doi.org/10.1016/j.jhazmat.2005.11.038.
[16] Afroughsabet V, Biolzi L, Monteiro PJM, Gastaldi MM. Investigation of the mechanical and durability properties of sustainable high performance concrete based on calcium sulfoaluminate cement. J Build Eng 2021;43:1–14. https://doi.org/10.1016/j.jobe.2021.102656.
[17] Enfedaque A, Gálvez JC, Suárez F. Analysis of fracture tests of glass fibre reinforced cement (GRC) using digital image correlation. Constr Build Mater 2015;75:472–87. https://doi.org/10.1016/j.conbuildmat.2014.11.031.
[18] Burris LE, Kurtis KE. Water-to-cement ratio of calcium sulfoaluminate belite cements: hydration, setting time, and strength development. Cement 2022;8:100032. https://doi.org/10.1016/j.cement.2022.100032.
[19] Sirtoli D, Wyrzykowski M, Riva P, Tortelli S, Marchi M, Lura P. Shrinkage and creep of high-performance concrete based on calcium sulfoaluminate cement. Cem Concr Compos 2019;98:61–73. https://doi.org/10.1016/j.cemconcomp.2019.02.006.
[20] Winnefeld F, Kaufmann J. Concrete produced with calcium sulfoaluminate cement – a potential system for energy and heat storage. In: First middle east conference on smart monitoring, assessment and rehabilitation of Civil Structures, Dubai, UAE: 2011.
[21] Dillard RJ, Murray CD, Deschenes RA. Belitic calcium sulfoaluminate cement subjected to sulfate attack and sulfuric acid. Constr Build Mater 2022;343:128089. https://doi.org/10.1016/j.conbuildmat.2022.128089.
[22] Jhatial AA, Kancir IV, Serdar M. Comparative study of selected properties of three binders: blended portland cement, calcium sulfoaluminate cement and alkali activated material based concrete. 2nd international conference on construction materials for sustainable future. 2021.
[23] Colonna D, Leone M, Aiello MA, Tortelli S, Marchi MI. Short and long-term behaviour of R.C. beams made with CSA binder. Eng Struct 2019;197:109370.
[24] Tang X, Xu Q, Qian K, Ruan S, Lian S, Zhan S. Effects of cyclic seawater exposure on the mechanical performance and chloride penetration of calcium sulfoaluminate concrete. Constr Build Mater 2021;303:124139. https://doi.org/10.1016/j.conbuildmat.2021.124139.
[25] Cook GW, Murray CD. Behavior of reinforced concrete made with belitic calcium sulfoaluminate cement at early ages. ACI Mater J 2020;117(1). https://doi.org/10.14359/51719074.
[26] Gartner E. Industrially interesting approaches to "low-CO_2" cements. Cem Concr Res 2004;34(9):1489–98. https://doi.org/10.1016/j.cemconres.2004.01.021.
[27] Trauchessec R, Mechling JM, Lecomte A, Roux A, Le Rolland B. Hydration of ordinary Portland cement and calcium sulfoaluminate cement blends. Cem Concr Compos 2015;56:106–14. https://doi.org/10.1016/j.cemconcomp.2014.11.005.
[28] Pelletier L, Winnefeld F, Lothenbach B. The ternary system Portland cement-calcium sulphoaluminate clinker-anhydrite: hydration mechanism and mortar properties. Cem Concr Compos 2010;32(7):497–507. https://doi.org/10.1016/j.cemconcomp.2010.03.010.
[29] Cau Dit Coumes C, Courtois S, Peysson S, Ambroise J, Pera J. Calcium sulfoaluminate cement blended with OPC: a potential binder to encapsulate low-level radioactive slurries of complex chemistry. Cem Concr Res 2009;39(9):740–7. https://doi.org/10.1016/j.cemconres.2009.05.016.
[30] Telesca A, Marroccoli M, Pace ML, Tomasulo M, Valenti GL, Naik TR. Expansive and non-expansive calcium sulfoaluminate-based cements. In: Third international conference on sustainable construction materials and technologies, Kyoto, Japan; 2013.
[31] Dachtar J. Calcium sulfoaluminate cement as binder for structural concrete. University of Sheffield; 2004.
[32] Sherman N, Beretka J, Santoro L, Valenti GL. Long-term behaviour of hydraulic binders based on calcium sulfoaluminate and calcium sulfosilicate. Cem Concr Res 1995;25(1):113–26. https://doi.org/10.1016/0008-8846(94)00119-J.
[33] Ioannou S, Chowdhury M, Badr A. Conformity of the performance of calcium sulfoaluminate cement based concretes to empirical models in current international design standards. Constr Build Mater 2022;326:126748. https://doi.org/10.1016/j.conbuildmat.2022.126748.
[34] CEB-FIP. fib Model Code for Concrete Structures. fib - fédération internationale du béton; 2010.
[35] EN 12350-2. Testing fresh concrete - Part 2: Slump test. European Standard; 2019.
[36] EN 12350-7. Testing fresh concrete - Part 7: Air content - pressure methods. European Standard; 2019.
[37] EN 12350-7. Testing fresh concrete - Part 7: Air content - pressure methods. European Standard; 2019.
[38] EN 12390-3. Testing hardened concrete - Part 3: compressive strength of test specimens. European Standard; 2019.
[39] EN 12390-13. Testing hardened concrete - Part 13: Determination of secant modulus of elasticity in compression. European Standard; 2013.
[40] Vasanelli E, Micelli F, Antonietta M, Plizzari G. Long term behavior of FRC flexural beams under sustained load. Eng Struct 2013;56:1858–67. https://doi.org/10.1016/j.engstruct.2013.07.035.
[41] Colonna D. Short and long term behaviour of structural and non-structural elements made with calcium sulfoaluminate cement. University of Salento; 2019.
[42] Li X, Grasley ZC, Garboczi EJ, Bullard JW. Modeling the apparent and intrinsic viscoelastic relaxation of hydrating cement paste. Cem Concr Compos 2015;55:322–30. https://doi.org/10.1016/j.cemconcomp.2014.09.012.
[43] Winnefeld F, Lothenbach B. Hydration of calcium sulfoaluminate cements - experimental findings and thermodynamic modelling. Cem Concr Res 2010;40(8):1239–47. https://doi.org/10.1016/j.cemconres.2009.08.014.